Supplementary Information

Dual Carbon Layers Hybridized Mesoporous Tin Hollow Spheres for Fast-rechargeable and High-stable Lithium-ion Battery Anode

Weili An, [a] Jijiang Fu, [a] Shixiong Mei, [a] Lu Xia, [a] Xingxing Li, [a] Huazhi Gu, [a] Xuming Zhang, [a,b] * Biao Gao, [a] * Paul K Chu, [b] and Kaifu Huo [c]

a. The State Key Laboratory of Refractories and Metallurgy, Wuhan University of Science and Technology, Wuhan 430081, China. E-mail: gaobiao@wust.edu.cn, xumzhang@wust.edu.cn; Tel.: +86-13517240510.

b. Department of Physics and Materials Science, City University of Hong Kong, Tat Chee Avenue, Kowloon, Hong Kong, China.

c. Wuhan National Laboratory for Optoelectronics (WNLO), School of Optical and Electronic Information Huazhong University of Science and Technology Wuhan 430074, China.

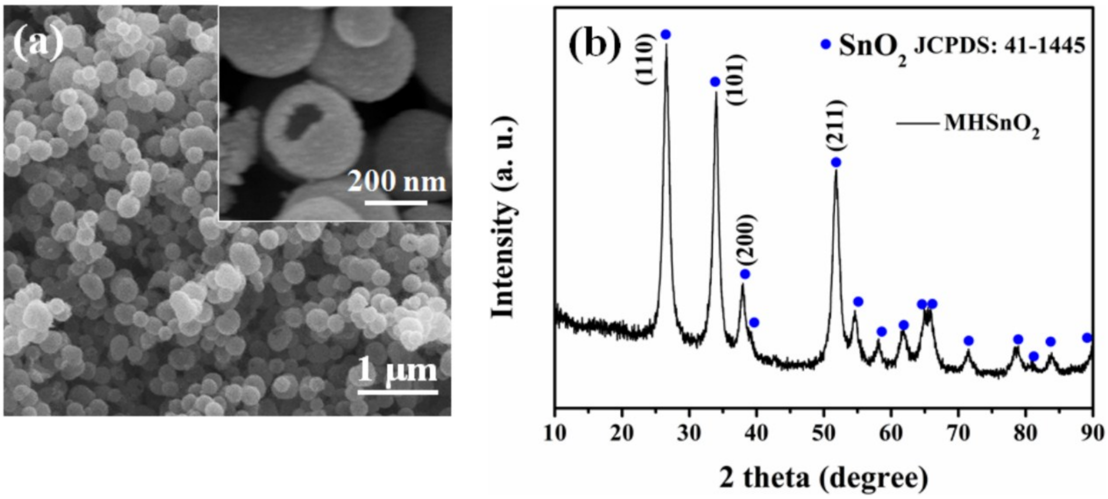

Fig. S1. (a) SEM image of $MHSnO_2$ with the inset being the magnified SEM image and **(b)** XRD pattern of $MHSnO_2$.

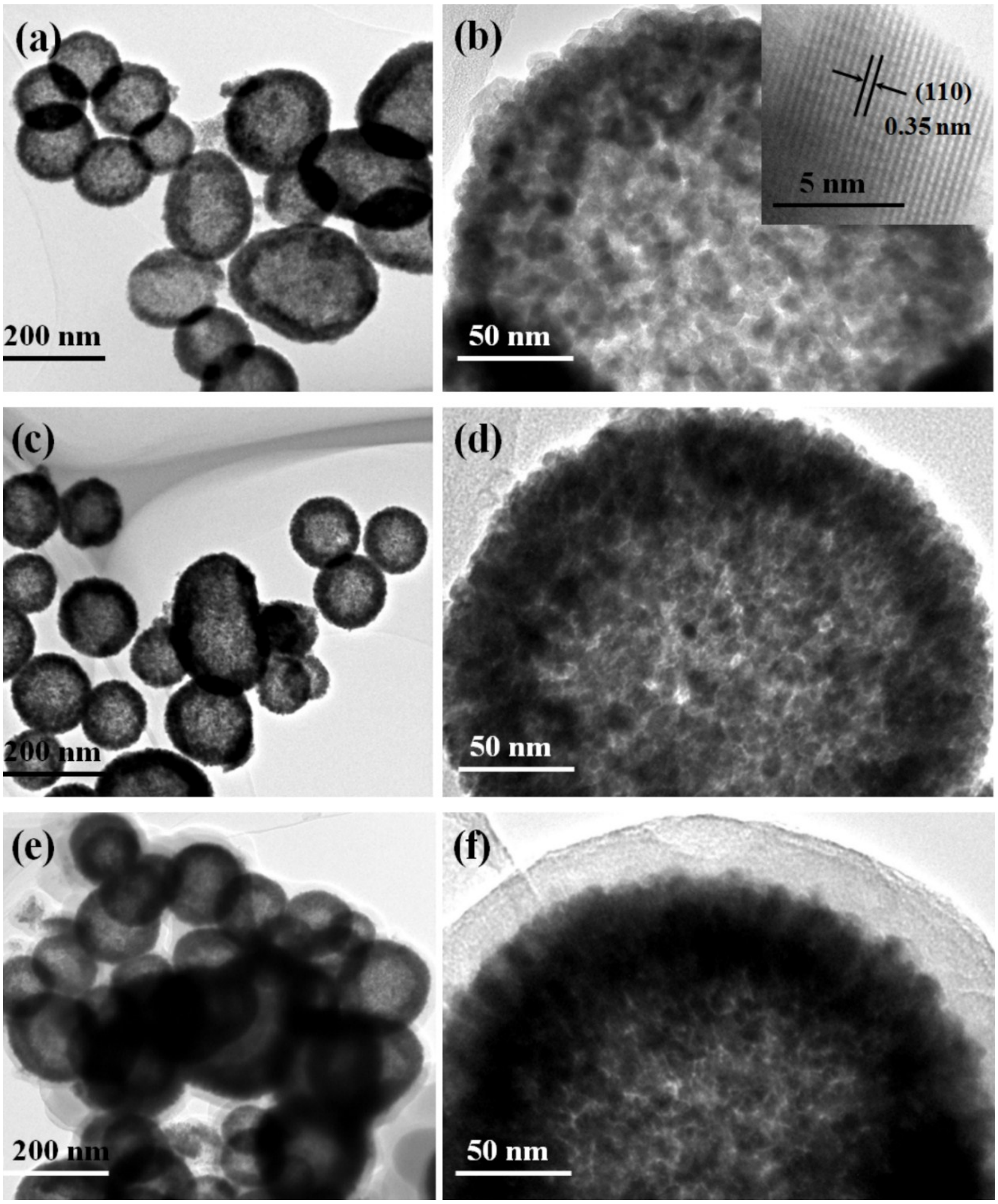

Fig. S2. TEM and HR-TEM images of (a, b) $MHSnO_2$, (c, d) $MHSnO_2$@PDA, and (e, f) $MHSnO_2$@PDA/PDA.

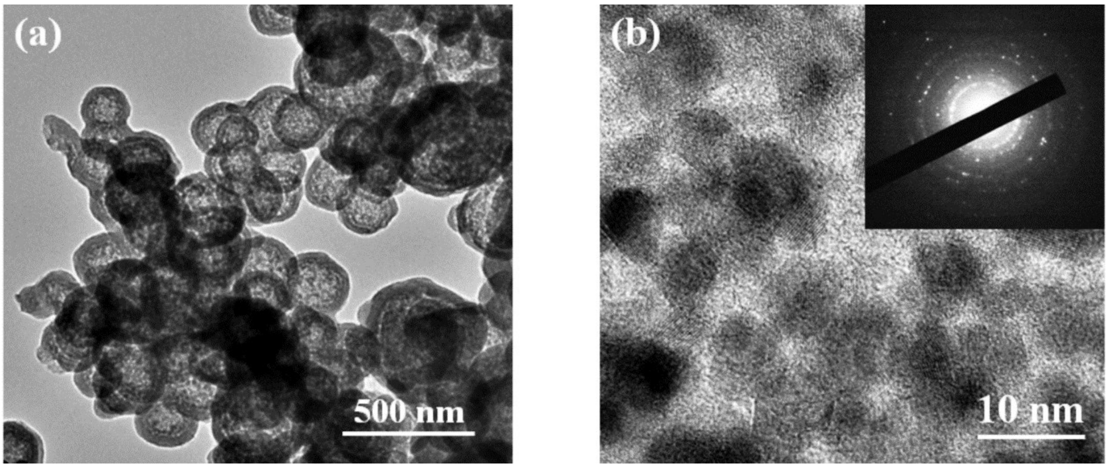

Fig. S3. (a) TEM image of MSHSs@C/C and (b) HR-TEM image showing the Sn NPs distribution in the shell of MSHSs@C/C with the inset being the SAED pattern.

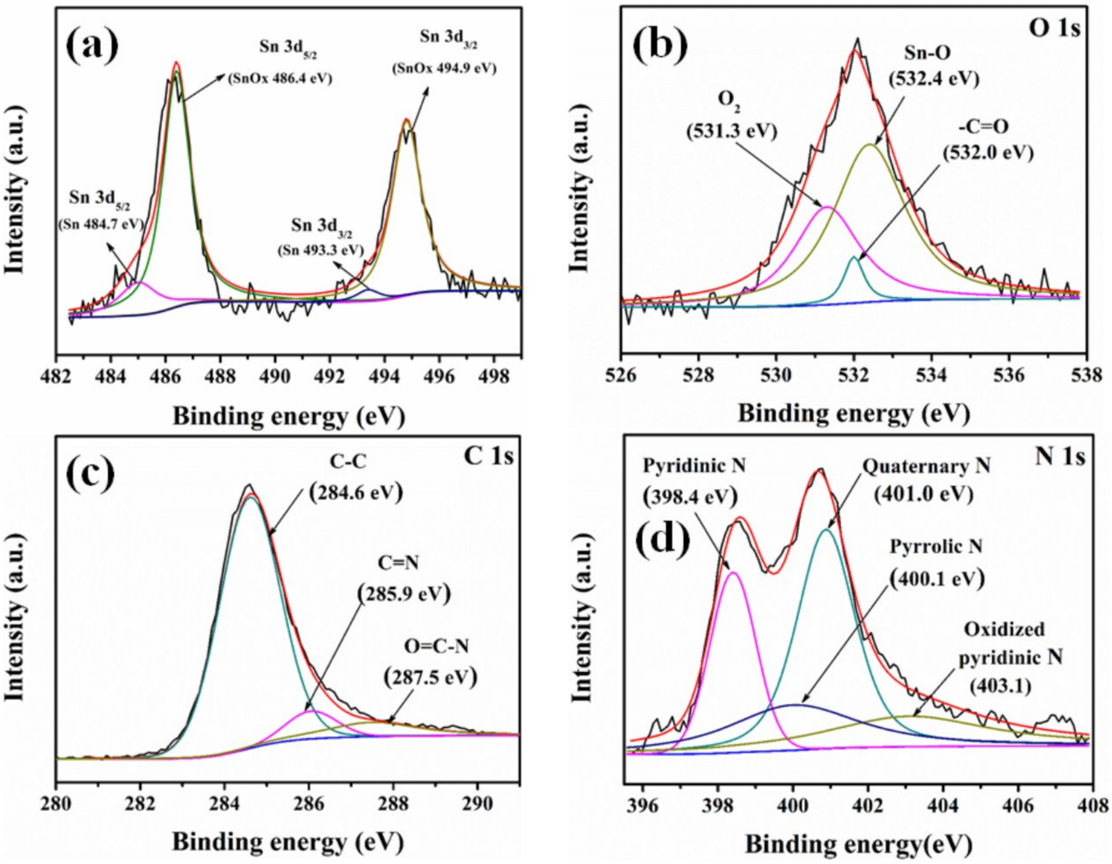

Fig. S4. High-resolution XPS spectra: (a) Sn 3d, (b) O 1s, (c) C 1s, (d) N 1s of MSHSs@C/C.

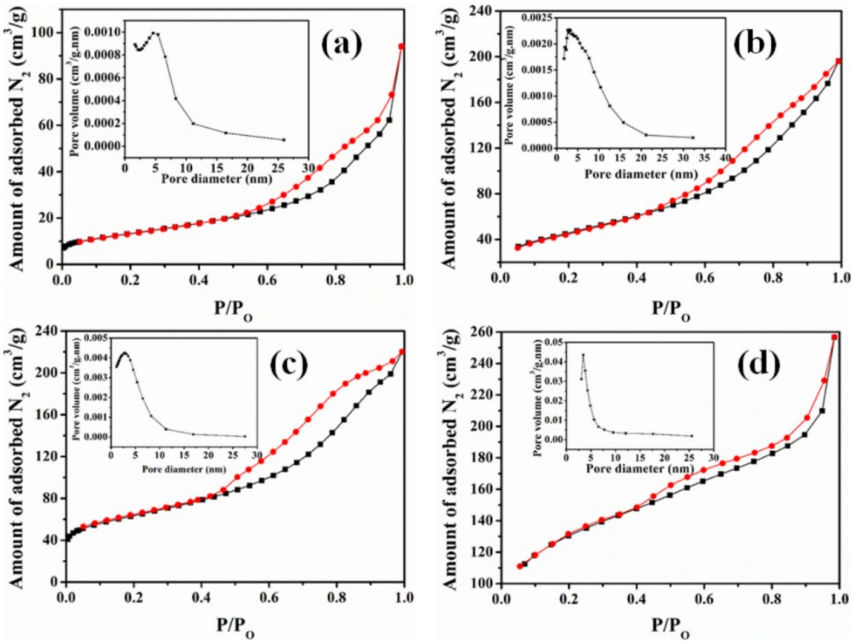

Fig. S5. Nitrogen adsorption-desorption isotherms of (a) $MHSnO_2$, (b) MSHSs@C (c) MSHSs@C/C, and (d) DCHSs with the insets showing the corresponding pore size distributions.

Table S1 Fitted impedance parameters of MSHSs, MSHSs@C, and MSHSs@C/C.

Sample	**Cycle**	**R_{Ω}**	**R_{sf}**	**R_{ct}**
MSHSs@C/C	500	5.12	21.35	53.15
MSHSs@C	500	6.77	40.87	118.45
MSHSs	500	7.39	—	139.3

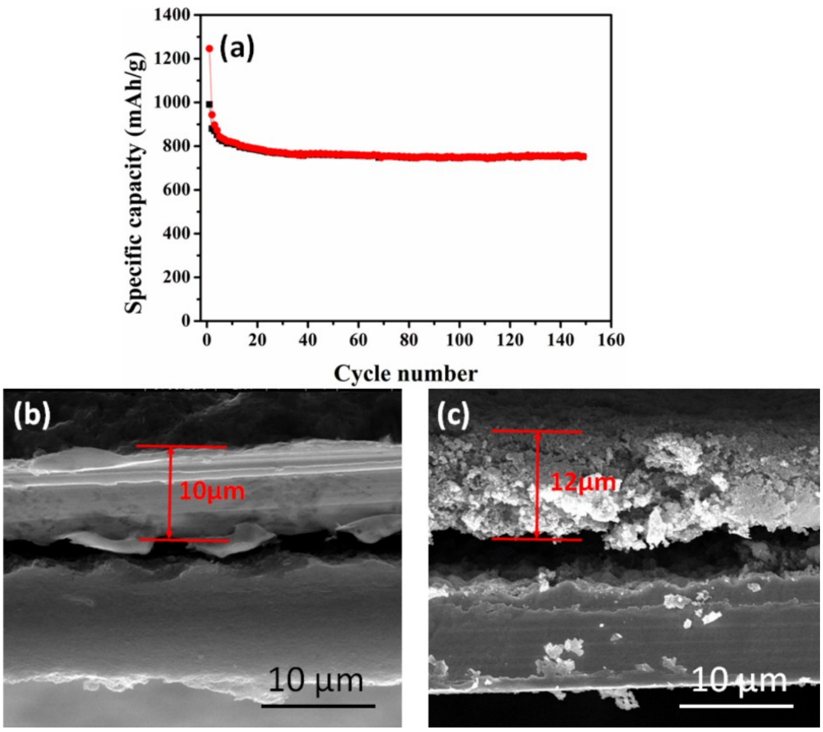

Fig. S6 Cycling performance (a) of MSHSs@C/C at low current density of 0.2 A g^{-1}; The top view SEM image about the thickness of slurry composite electrodes: primary electrode (b) and the electrode after 150 cycles at the voltage of 3.0 V (c).

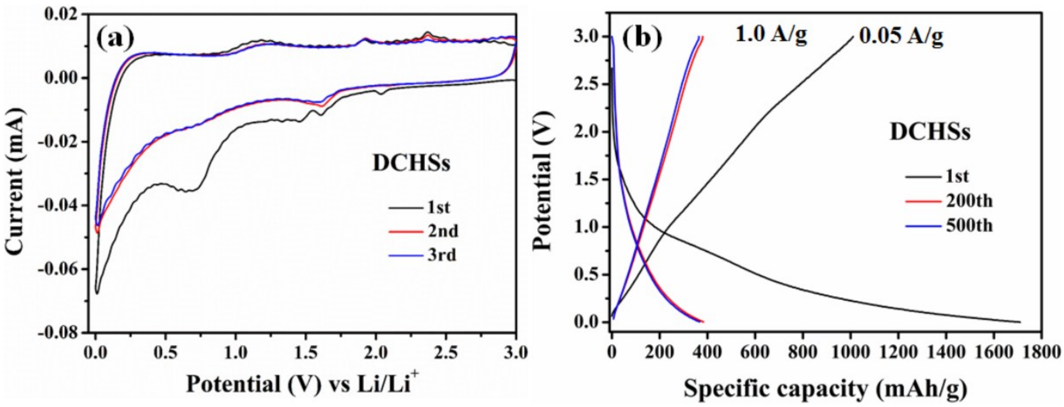

Figure S7 (a) Typical CV curves at a potential sweep rate of 0.1 mV s^{-1}; (b) Charge-discharge profiles at current density of 1.0 A g^{-1} of the N-doped carbon sphere electrode (DCHSs);

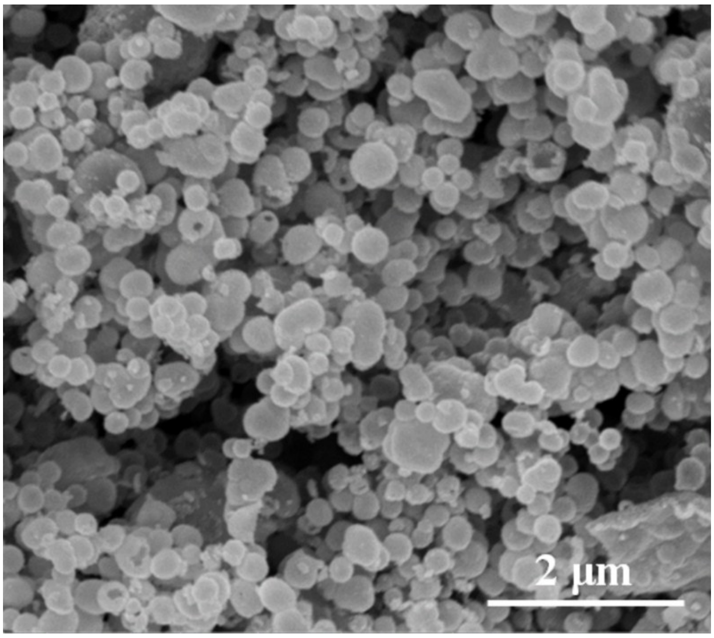

Fig. S8. SEM image of MSHSs without the PDA coating.

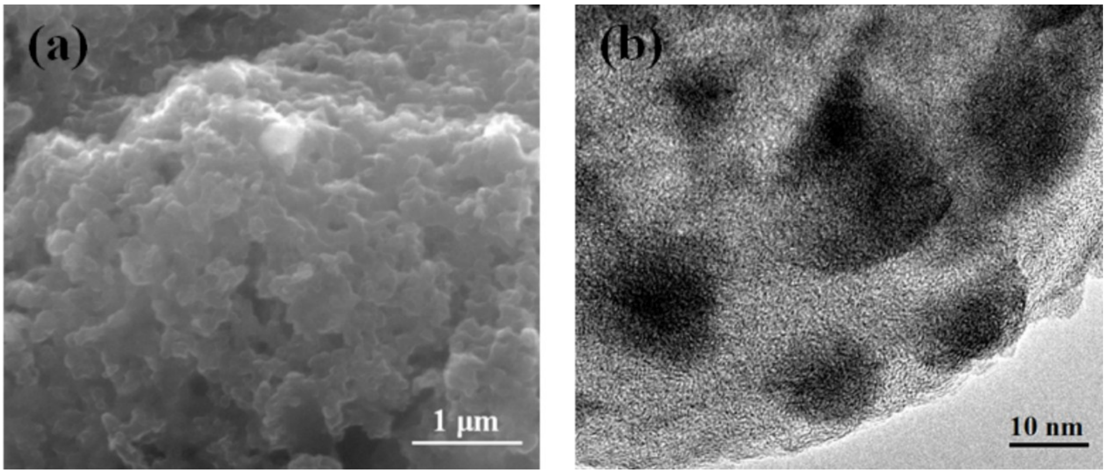

Fig. S9. (a) SEM image of MSHSs after 500 charging/discharging cycles; (b) HR-TEM image of MSHSs@C after full lithiation for 20 cycles.

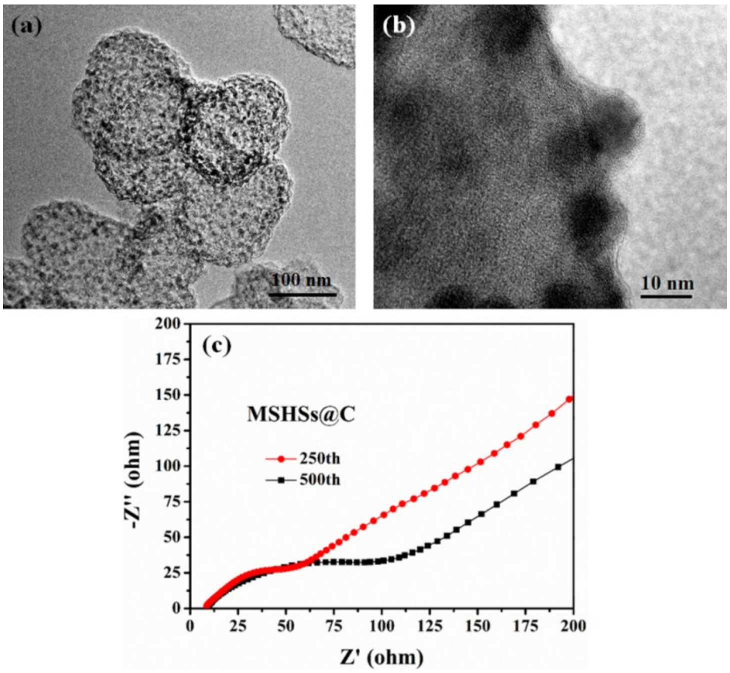

Fig. S10. (a) TEM and (b) HR-TEM images of MSHSs@C after 500 charging/discharging cycles; (c) Nyquist plots of MSHSs@C at the 250th and 500th cycles.

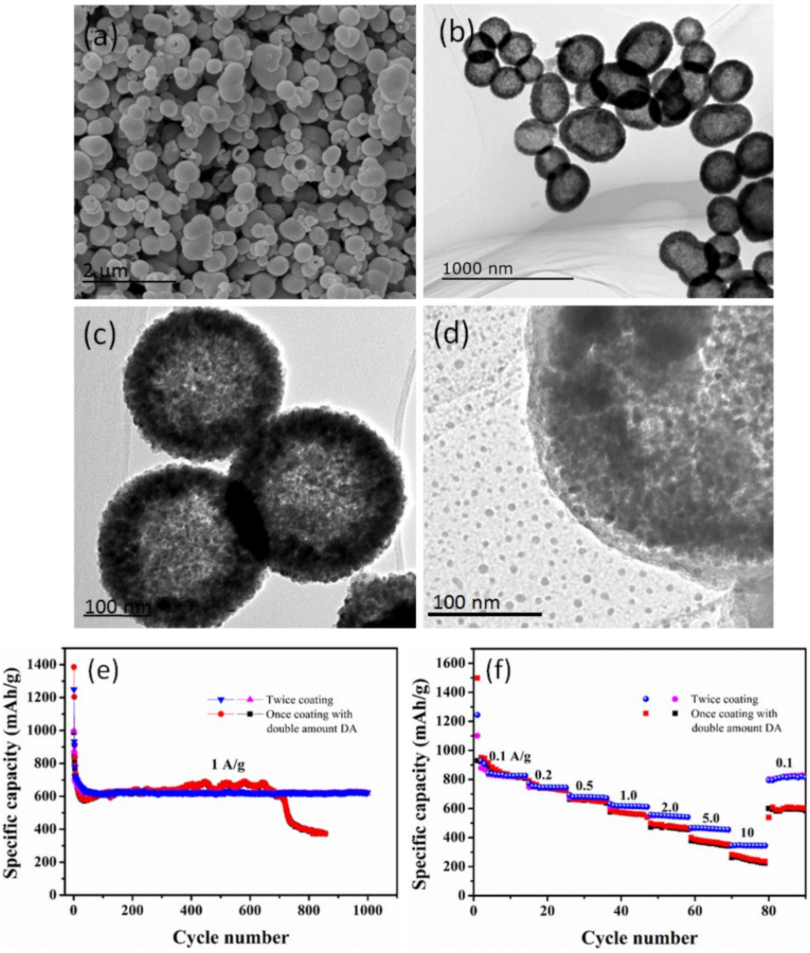

Figure S11. SEM (a), TEM (b) and magnified TEM (c) images of PDA coating SnO_2 hollow sphere (MHSnO_2@PDA-2) by one-step polymerization with double amount of dopamine hydrochloride; (d) HRTEM image of Sn/C hollow sphere (MSHSs@C-2) obtained from annealing PDA coated SnO_2 by one-step polymerization with double amount of dopamine; Cycling performance (e) and rate performance (f) of hollow Sn/C spheres by one-step polymerization with double amount of dopamine and two-step dopamine polymerization.

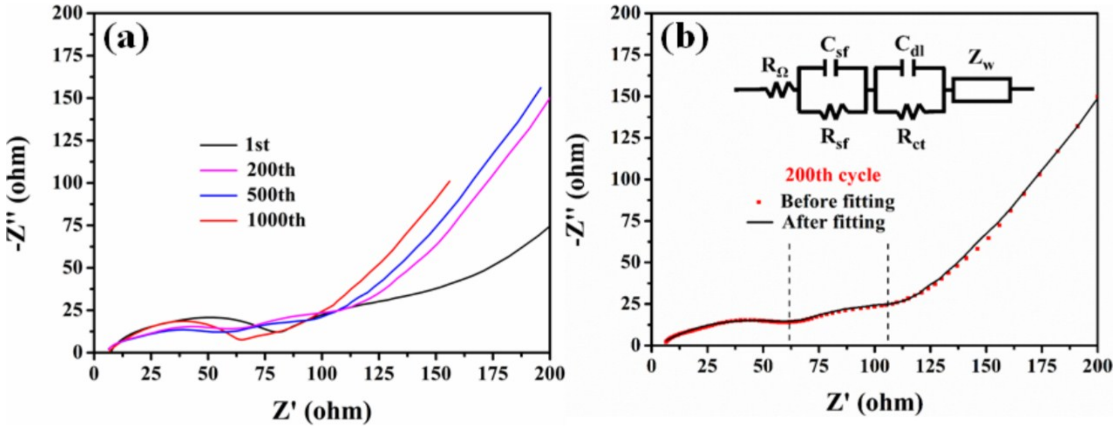

Fig. S12 (a) Nyquist plots of MSHSs@C/C for different cycles; (b) Fitted circuit after 200 cycles with the inset showing the modified equivalent circuit.

Table S2 Fitted impedance parameters at different cycles for MSHSs@C/C.

Sample	**Cycles**	$\mathbf{R_{\Omega}}$	$\mathbf{R_{sf}}$	$\mathbf{R_{ct}}$
MSHSs@C/C	1	2.81	45.63	88.4
	200	2.78	28.98	74.99
	500	5.12	21.35	53.15
	1000	6.04	24.04	43.19

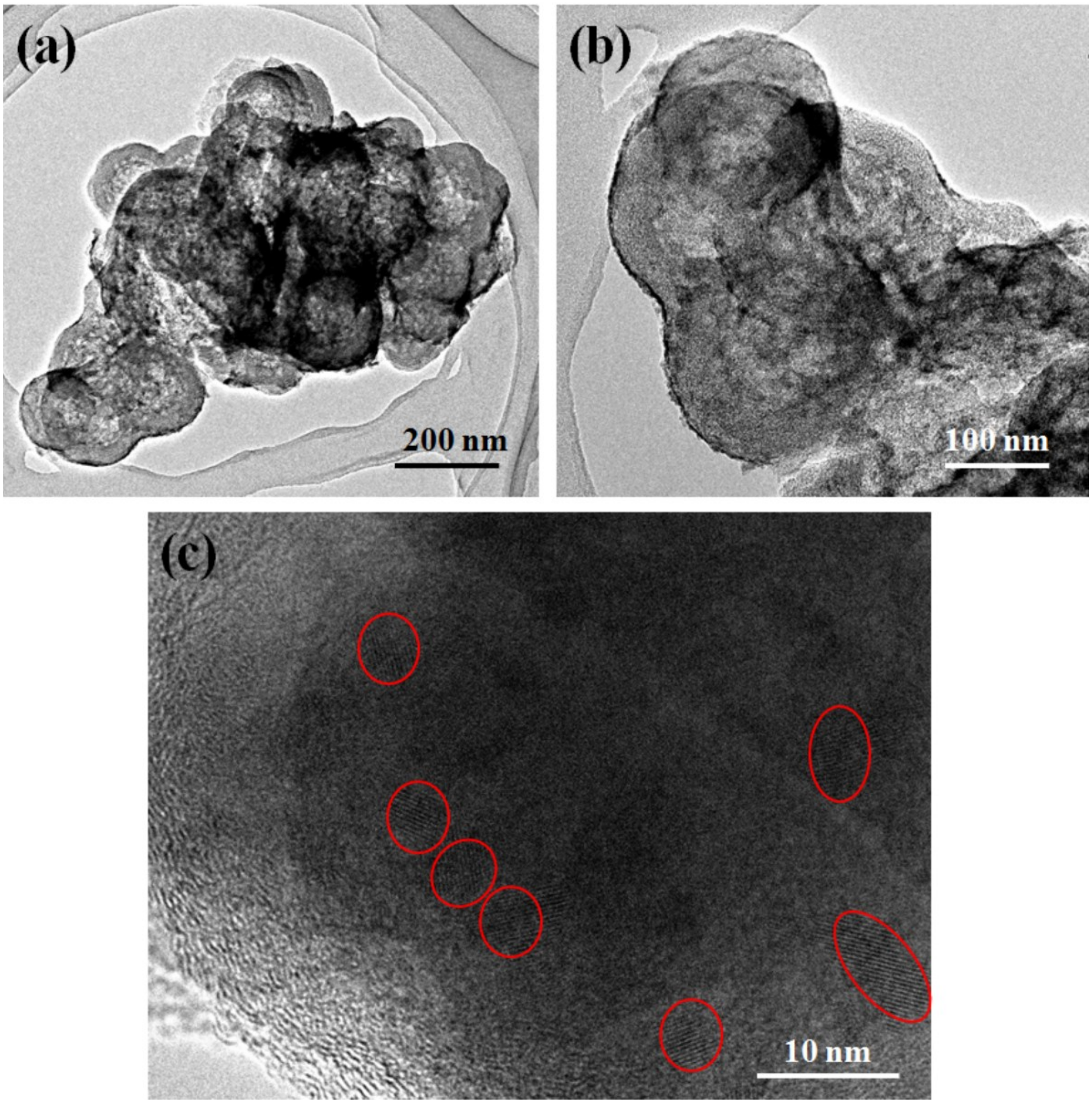

Fig. S13 (a, b) TEM and (c) HR-TEM images of MSHSs@C/C after long charging/discharging cycles at 10.0 A g^{-1}.